N-63-3-1

683 400

Final Report
Contract N140(70024)-72788B
December 1962

• applied • mathematics ••

Mathematical Methods in Transducer Field Theory: The Finite Cylinder

by

N. G. Parke III
W. Williams, Jr.

for

U. S. Navy Underwater Sound Laboratory

PARKE MATHEMATICAL LABORATORIES, Inc.
One River Road • Carlisle, Massachusetts

• pml • applied • mathematics •

SCIENTIFIC REPORTS

their purpose and place

•••A•P•P•L•I•E•D••M•A•T•H•E•M•A•T•I•C•I•A•N•S•••

THE EVER INCREASING NEED TO BE INFORMED has caused an ever increasing volume of publications. The very quantity of these publications, however, makes it difficult to satisfy the need, because it becomcs more and more arduous to locate the literature pertinent to any one subject; and because any one of us becomes more and more weary of having so much to read. Moreover, only a small minority of these publications may help satisfy the need, because an overwhelming majority is void of content.

Consequently, it is imperative to present to the public only manuscripts which do carry new information without undue verbiage; hoping to be judged not by the number of published pages but by their quality. In particular, papers in the field of Applied Mathematics ought to be published only if they contain one or more of the following items: new basic results, new methods, new applications, new numerical results, new presentation of difficult and important topics, up-to-date bibliographies; and if the number of their pages is not dictated by the desire of imposing upon the superficial reader.

To discharge our contractual obligations, we publish *Technical or Scientific Reports,* such as the one you now have in your hands. It has been our constant policy to see to it, that they satisfy the above strict criterion.

PARKE MATHEMATICAL LABORATORIES, INC.
carlisle, massachusetts

Final Report
Contract N140(70024)-72788B
December 1962

• • • applied • mathematics • •

Mathematical Methods in Transducer Field Theory: The Finite Cylinder

by

N. G. Parke III
W. Williams, Jr.

for

U. S. Navy Underwater Sound Laboratory

PARKE MATHEMATICAL LABORATORIES, Inc.
Bedford Road • Carlisle, Massachusetts

PARKE MATHEMATICAL LABORATORIES, INCORPORATED
ONE RIVER ROAD CARLISLE, MASSACHUSETTS

Requests for additional copies by Agencies of the Department of Defense, their contractors, and other Government agencies should be directed to the:

ARMED SERVICES TECHNICAL INFORMATION AGENCY
ARLINGTON HALL STATION
ARLINGTON 12, VIRGINIA

Department of Defense contractors must be established for ASTIA services or have their 'need-to-know' certified by the cognizant military agency of their project or contract.

All other persons and organizations should apply to the:

U.S. DEPARTMENT OF COMMERCE
OFFICE OF TECHNICAL SERVICES
WASHINGTON 25, D.C.

A limited number of copies are also available by writing to:

PARKE MATHEMATICAL LABORATORIES, INC.
ONE RIVER ROAD
CARLISLE, MASSACHUSETTS

TABLE OF CONTENTS

I. Introduction 1

II. Background 1

III. The Finite Cylinder Problem 2

A. General Theoretical Analysis 2

B. Numerical Analysis of a Specific Case 12

IV. Remarks 20

V. Arbitrary Finite Bodies of Revolution 23

VI. NOTE ADDED IN PROOF 24

Mathematical Methods in Transducer Field Theory: The Finite Cylinder

by

N. G. Parke III and W. Williams

Introduction

This report deals primarily with a method of determining the velocity potential for the sound field generated by a finite circular cylinder with rigid end faces which is executing pure radial, harmonic vibrations uniformly over its cylindrical surface; it will be concluded, following the presentation of a specific numerical calculation, with a simple extension of the method applicable to the determination of the velocity potential for the sound field generated by arbitrary finite bodies of revolution vibrating harmonically in time.

Background

As a consequence of specifying harmonic time dependence, the problem of determining the time dependent velocity potential $\Psi(\vec{r}, t)$ in a domain exterior to the vibrating source from the wave equation:

$$\nabla^2 \Psi(\vec{r}, t) - 1/c^2 \, \frac{\partial^2 \Psi(\vec{r}, t)}{\partial t^2} = 0 \tag{1}$$

(in which c is the sound speed) reduces, upon the usual substitution of

$$\Psi(\hat{r}, t) = Re\left\{ \psi(\hat{r}) e^{-i\omega t} \right\} \tag{2}$$

in (1) to the determination of the time independent velocity potential $\psi(\hat{r})$ in a domain exterior to the vibrating source from the Helmholtz equation:

$$\nabla^2 \psi(\hat{r}) + k^2 \psi(\hat{r}) = 0 \tag{3}$$

(in which the wave number $k = 2\pi/\lambda$ where λ is "the" wave length of the sonic radiation). Further, if the Sommerfeld radiation condition

$$\lim_{r \to \infty} r\left[\frac{\partial \psi(\hat{r})}{\partial r} - ik\psi(\hat{r}) \right] = 0, \tag{4}$$

is imposed upon $\psi(\hat{r})$ then an important paper by Hartman and Wilcox[1] shows that for a space of three dimensions the following series expansion converges in the mean to $\psi(\hat{r})$ in an exterior domain

$$(5) \qquad \psi(\hat{r}) \sim \sum_{\ell=0}^{\infty} \sum_{m=-\ell}^{m=+\ell} i^{\ell} a_{\ell m} h_{\ell}^{(1)}(kr) \cdot Y_{\ell m}(\theta, \varphi)$$

(in which $h_{\ell}^{(1)}$ is a spherical Hankel function of the first kind and $Y_{\ell m}$ is a spherical harmonic).

Hence, the problem of determining the time independent velocity potential $\psi(\hat{r})$ in domain exterior to a finite source of the sound field consists in the specification of the constants $a_{\ell m}$ subject to the application of appropriate boundary conditions.

The Finite Cyl··der Problem

General Theoretical Analysis - In order to specify the precise boundary conditions, the center of the circular cylinder of radius a and length $2b$ will be placed at the origin of a coordinate system in which either the cylindrical coordinate set ρ, z, φ or the spherical coordinate set r, θ, φ will be employed depending on efficacy. With the assertion of rigid (i.e., motionless) end faces and pure radial harmonic vibratory motion of the cylindrical surface, the boundary conditions on the finite cylinder, which follow directly from the relation between the velocity $\hat{v}$ and the time dependent velocity potential $\Psi(\hat{r}, t)$, $\hat{v} = \text{grad}\, \Psi(\hat{r}, t)$, can be written, apart from a scale factor, as

$$(6a) \qquad \frac{\partial \psi(\hat{r})}{\partial z} = 0 \qquad \text{on the end surfaces: } 0 \leq \rho \leq a; \quad z = \pm b$$

$$(6b) \qquad \frac{\partial \psi(\hat{r})}{\partial \rho} = 1 \qquad \text{on the cylindrical surface: } \rho = a; \ -b \leq z \leq +b$$

for the time independent velocity potential $\psi(\hat{r})$.

---

(1) Ph. Hartman and C. Wilcox, "On Solutions of the Helmholtz Equation in Exterior Domains", Math. Zeitschr., 75, 228-255 (1961).

Two immediate simplifications in the structure of the series expansion (5) for $\psi(\hat{r})$ follow immediately from symmetry considerations:

a) The specification of the cylinder as circular dictates azimuthal symmetry; consequently, $m=0$ in (5) and $Y_{\ell m}(\theta,\phi) \rightarrow Y_{\ell 0}(\theta,\phi) \rightarrow P_\ell(\theta)$ where $P_\ell(\theta)$ is the usual Legendre polynomial.

b) The form of the Neumann condition (6b) on the cylindrical surface dictates equatorial symmetry (i.e., symmetry around the plane $z=0$, $0 \leq \phi \leq 2\pi$ or, equivalently, the plane $\theta = \pi/2$, $0 \leq \phi \leq 2\pi$); consequently, $\psi(\rho, z) = \psi(\rho, -z) \rightarrow P_\ell(\cos\theta) = P_\ell(\cos(\pi-\theta)) \rightarrow \ell = 0, 2, 4, \ldots$.

Hence,

$$(7) \qquad \psi(\hat{r}) = \psi(r,\theta) \sim \sum_{n=0}^{\infty} a_n h_n(kr) \cdot P_n(\cos\theta) \qquad n = 2\ell, \text{ even}$$

(in which i^ℓ has been absorbed into a_n and where $h_n(kr)$ without the super script (1) will continue to designate the spherical Hankel function of the first kind), and the problem for the finite cylinder is reduced to the two dimensional problem - because of the azimuthal symmetry - of finding the complex coefficients $a_0, a_2, a_4, \ldots, a_{2\ell}$ which satisfy the Neumann conditions (6) on the rectangular, cross sectional boundary of the cylinder.

In order to facilitate the analytical development which is required to calculate the normal derivative of the series expansion of (7), evaluate it on the rectangular boundary and match this evaluated derivative to the "data" for the problem as given by the boundary conditions of (6), the polar equation of the rectangular boundary is derived as follows. Examination of Figure 1 shows that the rectangular boundary - and also the domain exterior to the cylinder - is naturally divided into three regions:

$$(8) \qquad \begin{aligned} &\text{Region I: } 0 \leq \theta \leq \theta_0 = \tan^{-1} a/b \\ &\text{Region II: } \theta_0 < \theta < \pi - \theta_0 \\ &\text{Region III: } \pi - \theta_0 \leq \theta \leq \pi \end{aligned}$$

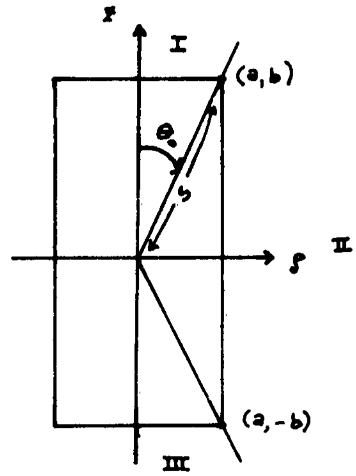

Figure 1 - Cross Section of Finite Cylinder

(in which the polar angle θ is measured from the positive z -axis) and that the radial distance from the coordinate origin to the boundary of the rectangular cross section is given in these separate regions by:

$$(9) \qquad \begin{aligned} &\text{Region I:} && r_{cyl} = b/\cos\theta \,, \\ &\text{Region II:} && r_{cyl} = a/\sin\theta \,, \\ &\text{Region III:} && r_{cyl} = -b/\cos\theta \,, \end{aligned}$$

where the negative sign is introduced in Region III in order to maintain $r>0$ in θ's second quadrant. If a discontinuous function, designated by us as an H-function[(2)], is introduced with the property for the variable x that

$$(10) \qquad H(\xi, \eta) = \begin{cases} 1 & \xi \leq x \leq \eta \\ 0 & \text{otherwise} \end{cases}$$

then the three polar equations for the rectangular boundary of (9) can be combined into the form

$$(11) \qquad r_{cyl} = b/\cos\theta \left[H(0,\theta_0) - H(\pi-\theta_0, \pi) \right] + a/\sin\theta \quad H(\theta_0^+, \pi-\theta_0^+)$$

(2) Which is the characteristic function of a set.

(in which $\theta_0^+ = \theta_0 + \epsilon$ where ϵ is infinitesimally small[3]). If the notation

$$H(0, \theta_0) \longrightarrow H_1(\theta) \longrightarrow H_1$$
$$H(\theta_0, \pi - \theta_0) \longrightarrow H_2(\theta) \longrightarrow H_2$$
$$H(\pi - \theta_0, \pi) \longrightarrow H_3(\theta) \longrightarrow H_3$$

is employed, then the polar equation for the boundary becomes

(12) $$r_{cyl} \longrightarrow s = b/\cos\theta \; (H_1 - H_3) + a/\sin\theta \; H_2 ,$$

which is the desired result.

In addition, the use of the H-functions leads immediately to the following expressions for ρ and z on the rectangular cross section

(13a) $$\rho = b \tan\theta \, (H_1 - H_3) + a H_2$$

(13b) $$z = b (H_1 - H_3) + a \cot\theta \, H_2$$

which, together with the obvious inter-regional property for the H-functions

(14) $$H_i H_j = \delta_{ij} H_j$$

(in which δ_{ij} is the Kronecker delta), leads to the relation

(15) $$s^2 = \rho^2 + z^2 = b^2/\cos^2\theta \; (H_1 + H_3) + a^2/\sin^2\theta \; H_2$$

which is, of course, also directly obtainable from (12).

The normal derivative $\frac{\partial\psi}{\partial n}$, which will be calculated over the boundary and then matched to the boundary conditions, has the form

(16) $$\frac{\partial\psi(r,\theta)}{\partial n} = (H_1 - H_3) \frac{\partial\psi(r,\theta)}{\partial z} + H_2 \frac{\partial\psi(r,\theta)}{\partial \rho}$$

(in which the negative sign is introduced to force the normal in the negative z direction in Region III). If, now, $\partial/\partial z$ and $\partial/\partial\rho$ are applied directly

---

[3] The distinction between θ_0 and θ_0^+ has been emphasized so that the regional definitions of (8) and the H-function definition of (10) are compatible; for practical calculation, however, such a distinction is an expensive luxury and will not be maintained.

to (7), thus yielding the normal derivative of the velocity potential in each region,

(17a) $$\frac{\partial\psi(r,\theta)}{\partial z} \sim \sum_{n=0}^{\infty} a_n \left\{ \frac{kz}{r} h_n'(kr) \cdot P_n(\cos\theta) + \frac{\rho \sin\theta}{r^2} h_n(kr) \cdot P_n'(\cos\theta) \right\}$$

(17b) $$\frac{\partial\psi(r,\theta)}{\partial \rho} \sim \sum_{n=0}^{\infty} a_n \left\{ \frac{k\rho}{r} h_n'(kr) \cdot P_n(\cos\theta) - \frac{z \sin\theta}{r^2} h_n(kr) \cdot P_n'(\cos\theta) \right\}$$

Then, substitution of (17) into (16) produces

$$\frac{\partial\psi}{\partial n} \sim \sum_{n=0}^{\infty} a_n \left\{ [(H_1 - H_3)z + H_2\rho]\frac{k}{r} h_n' P_n + [(H_1 - H_3)\rho - H_2 z]\frac{\sin\theta}{r^2} h_n P_n' \right\} \qquad n, \text{ even}$$

(in which the **prime indicates differentiation** with respect to the arguments-which have been suppressed temporarily-of either the Hankel function or Legendre polynomial). Evaluating this on the surface of the boundary by inserting the values of z and ρ from (13), and multiplying and dividing by s^2 leads immediately to

(18a) $$N(\theta) = \left.\frac{\partial\psi(\theta)}{\partial n}\right|_{cylinder} \sim \sum_{n=0}^{\infty} a_n f_n(\theta)/s^2 \qquad n, \text{ even}$$

where, the finite cylinder wave function $f_n(\theta)$ is given by

(18b) $$f_n(\theta) = k\left[\frac{b^2}{\cos\theta}(H_1 - H_3) + \frac{a^2}{\sin\theta} H_2\right] h_n'(ks) \cdot P_n(\cos\theta) + \left[\frac{b \sin^2\theta}{\cos\theta}(H_1 + H_3) - a \cos\theta\, H_2\right] h_n(ks) \cdot P_n'(\cos\theta)$$

which reduces upon substituting s from (12) to

(19a) Region I:
$$f_n^{(I)}(\theta) = b\left\{ \frac{kb}{\cos\theta} h_n'\left(\frac{kb}{\cos\theta}\right) \cdot P_n(\cos\theta) + \frac{\sin^2\theta}{\cos\theta} h_n\left(\frac{kb}{\cos\theta}\right) \cdot P_n'(\cos\theta) \right\}$$

(19b) Region II:
$$f_n^{(II)}(\theta) = a\left\{ \frac{ka}{\sin\theta} h_n'\left(\frac{ka}{\sin\theta}\right) \cdot P_n(\cos\theta) - \cos\theta\, h_n\left(\frac{ka}{\sin\theta}\right) \cdot P_n'(\cos\theta) \right\}$$

(19c) Region III:
$$f_n^{(III)}(\theta) = b\left\{ -\frac{kb}{\cos\theta} h_n'\left(-\frac{kb}{\cos\theta}\right) \cdot P_n(\cos\theta) + \frac{\sin^2\theta}{\cos\theta} h_n\left(-\frac{kb}{\cos\theta}\right) \cdot P_n'(\cos\theta) \right\}$$

The behavior of the simplest of these wave functions, namely, that of order $n = 0$ is exhibited in Figure 2[4] in which the real part of the wave function is plotted against the imaginary part. It should be pointed out that: for even n, $f_n^{I}(\theta) = f_n^{III}(\pi - \theta)$ and $f_n^{II}(\theta) = f_n^{II}(\pi - \theta)$ i.e., the wave functions are even with respect to $\theta = \pi/2$ and for odd n, $f_n^{I}(\theta) = -f_n^{III}(\pi - \theta)$ and $f_n^{II}(\theta) = -f_n^{II}(\pi - \theta)$ i.e., the wave functions are odd with respect to $\theta = \pi/2$.

Hence, if the Neumann conditions of (6) are inserted into $N(\theta)$, the normal derivative of the velocity potential on the boundary, it is readily seen from (16) that

$$(20) \quad N(\theta) = \left.\frac{\partial \varphi(\theta)}{\partial n}\right|_{cylinder} = (H_1 - H_3) \left.\frac{\partial \varphi(\theta)}{\partial z}\right|_{cylinder} + H_2 \left.\frac{\partial \varphi(\theta)}{\partial \rho}\right|_{cylinder} \to H_2$$

and, therefore, that the complex coefficients $a_0, a_2, \ldots, a_n$ can be determined, <u>in principle</u>, from the relation

$$(21) \quad N(\theta) = H_2 \sim \sum_{n=0}^{\infty} a_n f_n(\theta)/s^2 = \sum_{n=0}^{\infty} a_n \phi_n(\theta) \qquad n, \text{ even}$$

(in which $\phi_n(\theta) = f_n(\theta)/s^2$) thus solving the finite cylinder problem, <u>in principle</u>. Unfortunately, however, it is not possible to follow the usual procedure of determining the coefficients of a general Fourier expansion and develop an exact expression for the coefficient a_n in terms of an integral involving $\phi_n^*(\theta)$ and $N(\theta)$ since different $\phi_n(\theta)$'s are not orthogonal in the $0 \leq \theta \leq \pi$ interval[5]. Therefore, a weighted least squares procedure which leads to approximate values for the coefficients a_n and, thus, to an approximate solution for the finite cylinder problem has been utilized.

The calculation consists in approximating the infinite series $N(\theta)$ of

---

[4] For this purpose the following numerical assignments have been made $ka = 5$, $a = 1$, $b = 2$; these assignments are maintained in all subsequent numerical calculations.

[5] This is readily verified after some numerical analysis by plotting the product of $\phi_m^*(\theta)\phi_n(\theta)$ for $m \neq n$ against the polar angle θ . If $\phi_n(\theta)$ is orthogonal to $\phi_m(\theta)$, then the areas under the real and the imaginary parts of the product function must vanish separately; this did not occur in the case $m = 0$, $n = 2$ for example.

Figure 2 *Finite Cylinder Wave Function for n = 0*

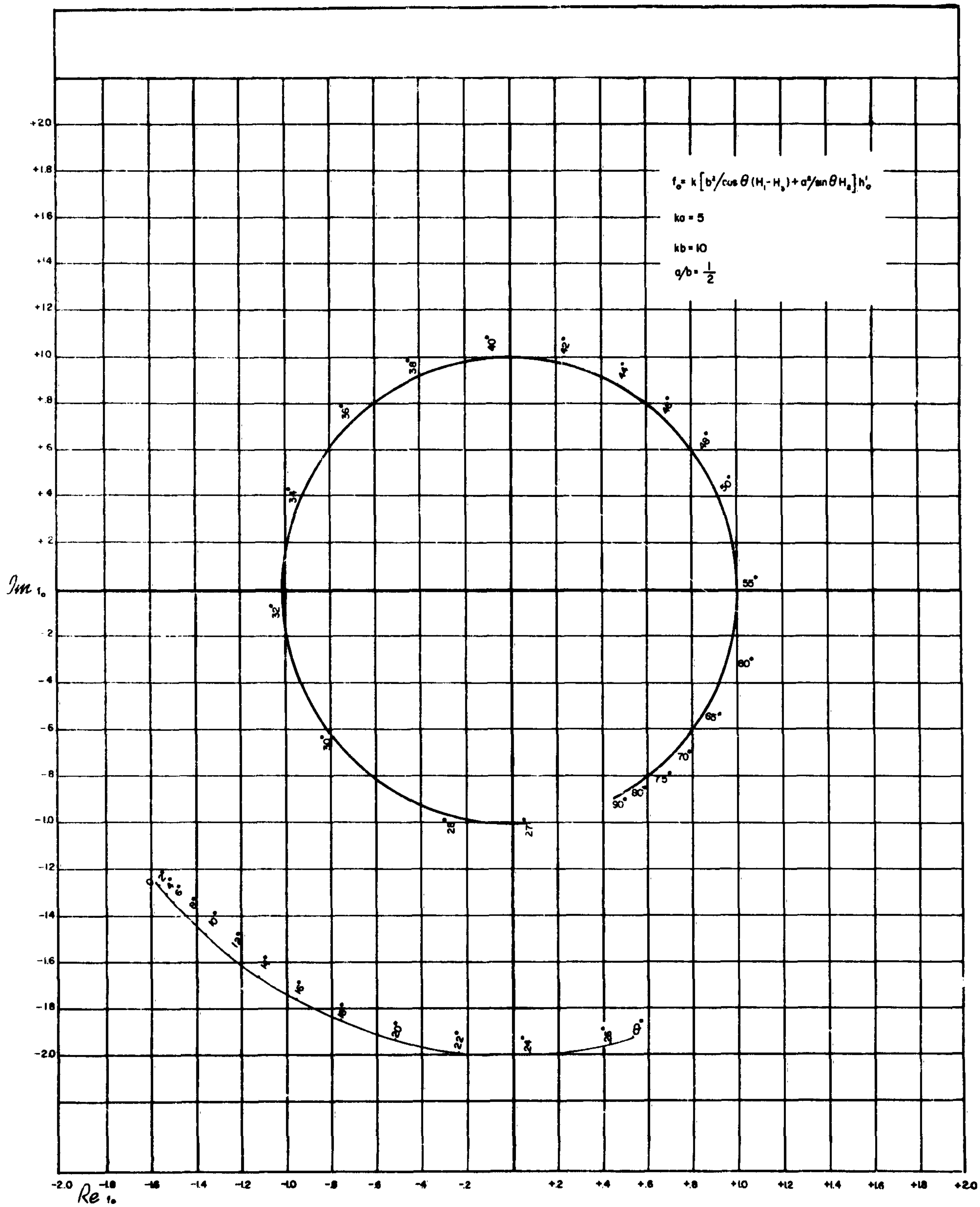

(21) by a finite series $G(\theta)$ of the form

(22a) $$G(\theta) = \sum_{n=0}^{N} a_n \phi_n(\theta),$$

and requiring that the weighted average value of the square of the misfit be a minimum with respect to the choice of the coefficients a_n on the boundary. That is, the "misfit integral"

(22b) $$E = \int_0^{\pi} [N(\theta) - G(\theta)]^2 \, W(\theta) \, d\theta$$

(in which $W(\theta)$ is a suitably chosen weighting function) is to be minimized with respect to the choice of a_k by means of the requirement that

(22c) $$\frac{\partial E}{\partial a_k} = 0.$$

Since, the $\phi_n(\theta)$ are in general complex because of the presence of the Hankel functions and their first derivatives in the $f_n(\theta)$, the symmetric form of (22b) must be employed which, when combined with (22a) and (22c), yields

(23a) $$\frac{\partial}{\partial a_k} \left\{ \int_0^{\pi} \left[N(\theta) - \sum_{n=0}^{N} a_n \phi_n(\theta) \right] \left[N^*(\theta) - \sum_{m=0}^{N} a_m^* \phi_m^*(\theta) \right] W(\theta) \, d\theta \right\} = 0$$

or, carrying out the indicated operations and noting that $\frac{\partial a_i}{\partial a_j} = \delta_{ij}$ and $\frac{\partial a_i^*}{\partial a_j} = 0$,

(23b) $$\int_0^{\pi} \left\{ -N^*(\theta) \sum_{n=0}^{N} \delta_{nk} \phi_n(\theta) + \sum_{n=0}^{N} \sum_{m=0}^{N} \delta_{nk} a_m^* \phi_n(\theta) \phi_m^*(\theta) \right\} W(\theta) \, d\theta = 0.$$

By substituting $N^*(\theta) = N(\theta) = H_2$ and inverting the order of summation and integration, (23b) becomes the set of $\frac{N}{2} + 1$ equations

(24a) $$\sum_{m=0}^{N} a_m^* \left\{ \int_0^{\pi} \phi_m^*(\theta) \phi_k(\theta) W(\theta) \, d\theta \right\} = \int_0^{\pi} H_2 \, \phi_k(\theta) W(\theta) \, d\theta$$

or equivalently,

$$\sum_{n=0}^{N} a_n \left\{ \int_0^{\pi} \phi_k^*(\theta)\, \phi_n(\theta)\, W(\theta)\, d\theta \right\} = \int_0^{\pi} H_2 \phi_k^*(\theta)\, W(\theta)\, d\theta, \qquad n, k \text{ even} \tag{24b}$$

which are the N relationships required to calculate the "best" approximate coefficients $a_0, a_2, \ldots, a_N$ once a suitable weight function is selected[6].

The choice of a particular weight function $W(\theta)$ can not be made on an a priori analytic basis but rather must be made by an appeal to the physics of the problem. If the Riemann integral on the right-hand side of (24b) is cast temporarily as a Stieltjes integral[7] over the boundary surface

$$\int_0^{\pi} H_2\, \phi_k^*(\theta)\, W(\theta)\, d\theta \longrightarrow \int_S H_2 \phi_k^*(\theta)\, dW \tag{25}$$

then, clearly, dW weights $\phi_k^*(\theta)$ as some function, not yet defined, of the boundary surface. Consequently, in view of the fact that no preference for any portion of the surface at the expense of some other portion is inherent in the original formulation of the problem, the appropriate selection appears to be that of weighting the $\phi_k^*(\theta)$ with respect to an element of surface in a manner independent of the element's position, that is

$$dW \longrightarrow d(\text{surface}), \tag{26a}$$

or, since the surface is a surface of revolution

$$dW = 2\pi s \cdot \sin\theta \sqrt{s^2 + \left(\frac{ds}{d\theta}\right)^2}\; d\theta \;. \tag{26b}$$

If, the indicated operations are performed with (12) and (15), then

$$dW = 2\pi \left[\frac{b^2 \sin\theta}{\cos^3\theta} (H_1 \pm H_3) \pm \frac{a^2}{\sin^2\theta} H_2 \right] d\theta \tag{27a}$$

(6) It should be noted in passing that if the $\phi_n(\theta)$ are orthogonal with respect to the weighting function $W(\theta)$, then (24a) reduces to the usual formula for the determinating of the Fourier coefficient a_k^*.

(7) Admittedly the introduction of a Stieltjes integral is not necessary because of the presence of the H-functions; this form does, however, possess a certain aesthetic appeal in view of the three sharply defined boundary regions.

where the ambiguity in the signs caused by taking the root can be removed either by formally requiring that

(27b) $$\int_{\text{surface}} dW = 2\pi a^2 + 4\pi a b$$

or by noting that since area is positive and the cosine and sine are odd and even, respectively, around $\theta = \pi/2$, that

(28) $$dW = W(\theta)\, d\theta = 2\pi\left[\frac{b^2 \sin\theta}{\cos^3\theta}(H_1 - H_3) + \frac{a^2}{\sin^2\theta} H_2\right] d\theta\,.$$

Hence, if the $W(\theta)$ of (28) is substituted into (24b), then the $N/2+1$ equations for the coefficients $a_0, a_2, \ldots a_N$ become

(29a) $$\sum_{n=0}^{N} a_n I_{k^*,n} = j_{k^*} \qquad k, n = 0, 2, 4, \ldots, N.$$

where

(29b) $$I_{k^*n} = 2\pi \int_0^{\pi} f_k^*(\theta)\, f_n(\theta) \left\{ \frac{\frac{b^2 \sin\theta}{\cos^3\theta}(H_1 - H_3) + \frac{a^2}{\sin^2\theta} H_2}{\frac{b^4}{\cos^4\theta}(H_1 + H_3) + \frac{a^4}{\sin^4\theta} H_2} \right\} d\theta,$$

and

(29c) $$j_{k^*} = 2\pi \int_0^{\pi} H_2\, f_k^*(\theta) \left\{ \frac{\frac{b^2 \sin\theta}{\cos^3\theta}(H_1 - H_3) + \frac{a^2}{\sin^2\theta} H_2}{\frac{b^2}{\cos^2\theta}(H_1 + H_3) + \frac{a^2}{\sin^2\theta} H_2} \right\} d\theta$$

(in which the $\phi_n(\theta)$ of (24b) have been replaced by $f_n(\theta)/s^2$, the $f_n(\theta)$ being given by (18b)). By splitting the single integrals into three region integrals and making use of the fact that the $f_n(\theta)$ are even with respect to $\theta = \pi/2$ for even n, it is seen that

(30a) $$I_{k^*n} = 2/b^2 \int_0^{\theta_0} f_k^{*(I)}(\theta)\, f_n^{(I)}(\theta) \sin\theta \cos\theta\, d\theta + 2/a^2 \int_{\theta_0}^{\pi/2} f_k^{*(II)}(\theta)\, f_n^{(II)}(\theta) \sin^2\theta\, d\theta$$

and

(30b) $$j_{k^*} = 2 \int_0^{\pi/2} f^{(2)*}_{k}(\theta)\, d\theta$$

where the factor of $2\pi_{(2)}$ common to $I^{(2)}_{k^*n}$ and j_{k^*} has been eliminated and where the specific forms of $f_n(\theta)$ and $f_n(\theta)$ are given by (19a) and (19b), respectively.

Because the structure of the integral I_{k^*n} of (30a) leads to the relationship that

(31) $$I_{\beta^*\alpha} = (I_{\alpha^*\beta})^*$$

where α and β are arbitrary even values of k and n, only slightly more than half of the $(N/2+1)^2$ integrals required by (29a) must be evaluated. Further, this property means, since (29a) can be regarded as the matrix equation

(32) $$\langle a \rangle \langle I \rangle = \langle j \rangle ,$$

(in which the complex a_n's are the elements of the row vector $\langle a \rangle$, the complex j_{k^*}'s are the elements of the row vector $\langle j \rangle$ and the complex $(I_{k^*n})^*$ are the elements of the coefficient matrix $\langle I \rangle$) that $\langle I \rangle$ is Hermitian. Hence, the inversion of equation (32), or equivalently, (29a) can be accomplished readily by means of the technique - fully described in Frazer[(8)] - of triangularizing the matrix $\langle I \rangle$ followed by successive backward substitutions of the a_n's into the resulting $N/2+1$ equations for the a_n, which completes the approximate solution of the finite cylinder problem.

Numerical Analysis of a Specific Case - Based on the theoretical development of the preceding section, the following numerical calculations for a three term series expansion $(N=4)$ were performed for the specific case $ka = 5$ (i.e. $\lambda = 2\pi a/5$), $a = 1$ and $b = 2$:

1. The individual wave functions $f_n(\theta)$ were calculated for $n = 0, 2$ and 4 ; a graphical representation of the calculation for $n = 0$ is found in Figure 2 which was inserted after the defining equations of (19).

(8) Frazer, R.A., Duncan, W.J. and Collar, A.R., Elementary Matrices, Cambridge Univ. Press, 1946. pp.97 et seq.

2. The integrals of (30a) and (30b) were evaluated by calculating the real and imaginary parts of their integrands, plotting these as a function of the polar angle θ and calculating the areas under these curves by means of repeated planimeter tracings. These results are given in Tables Ia and Ib:

k \ n	0	2	4
0	1.766	$-.014 - .235i$	$-.089 + .022i$
2	$-.015 + .233i$	.3494	$-.13056 - .0475i$
4	$-.087 - .027i$	$-.13037 + .0445i$	.1847

Table Ia - The I_{k^*n}.

k	j_{k^*}
0	$.9362 - .475i$
2	$.447 - .061i$
4	$.064 + .020i$

Table Ib - The j_{k^*}.

3. The complex coefficients of the three term series expansion of (29a) were determined by triangularizing the coefficient matrix $\langle I \rangle$ followed by the successive backward substitutions of a_4 and a_2 into the resulting three equations for a_0, a_2 and a_4. The results of this calculation are contained in Table II:

n	a_n
0	$.74 + .062\,i$
2	$2.2 + .75\,i$
4	$2.1 - .902\,i$

Table II – The a_n.

As a check on the ability of these values to fit the boundary condition data of (6), the real and imaginary contributions to the square root of the weighted "misfit" integrand of (22b) were calculated as a function of the polar angle θ.[9] The results of these calculations are presented graphically in Figure 3 where it should be noted that the extent of the "misfits" is quite satisfactory since a three term expansion is, admittedly, not sufficiently extensive to fit the discontinuous data under consideration with great "precision".

From these values for a_0, a_2 and a_4, a measure of the spatial distribution of maximum pressure in the sound field is obtained readily for this specific case since, apart from a scale factor, $P_{max}(\hat{r}) \sim |\psi(\hat{r})|$.[10] These results are shown graphically in Figures 4a, 4b and 4c for the three cases: $r = s$ (i.e., on the cylinder), $r = 2.5a$ and $r = 5a$, respectively.

The presence of the pressure "spike" on both the upper and lower end of the cylinder can be accounted for by examination of Figure 5 where the velocity or, equivalently, $\frac{\partial \psi(\hat{r})}{\partial n}$, which has been plotted against the polar angle, is observed to have a non-zero value in these two regions. This velocity

(9) In these calculations, the factor of 2π was not taken into account since it is a factor which could have been made to disappear immediately in (23a).

(10) This follows immediately from the relation $P(\hat{r},t) = -\rho \frac{\partial \Psi(\hat{r},t)}{\partial t}$ and the ansatz of (2), that is, $P(\hat{r},t) = Re\{i\omega\rho\,\psi(\hat{r})e^{-i\omega t}\} = Re\{i\omega\rho|\psi(\hat{r})|e^{i\alpha} \cdot e^{i\omega t}\}$ where the phase angle α is given by $\alpha = \tan^{-1}\{Re\,\psi(\hat{r})/Im\,\psi(\hat{r})\}$; hence, neglecting the scale factor and the phased time dependence, $P_{max}(\hat{r}) \sim |\psi(\hat{r})|$.

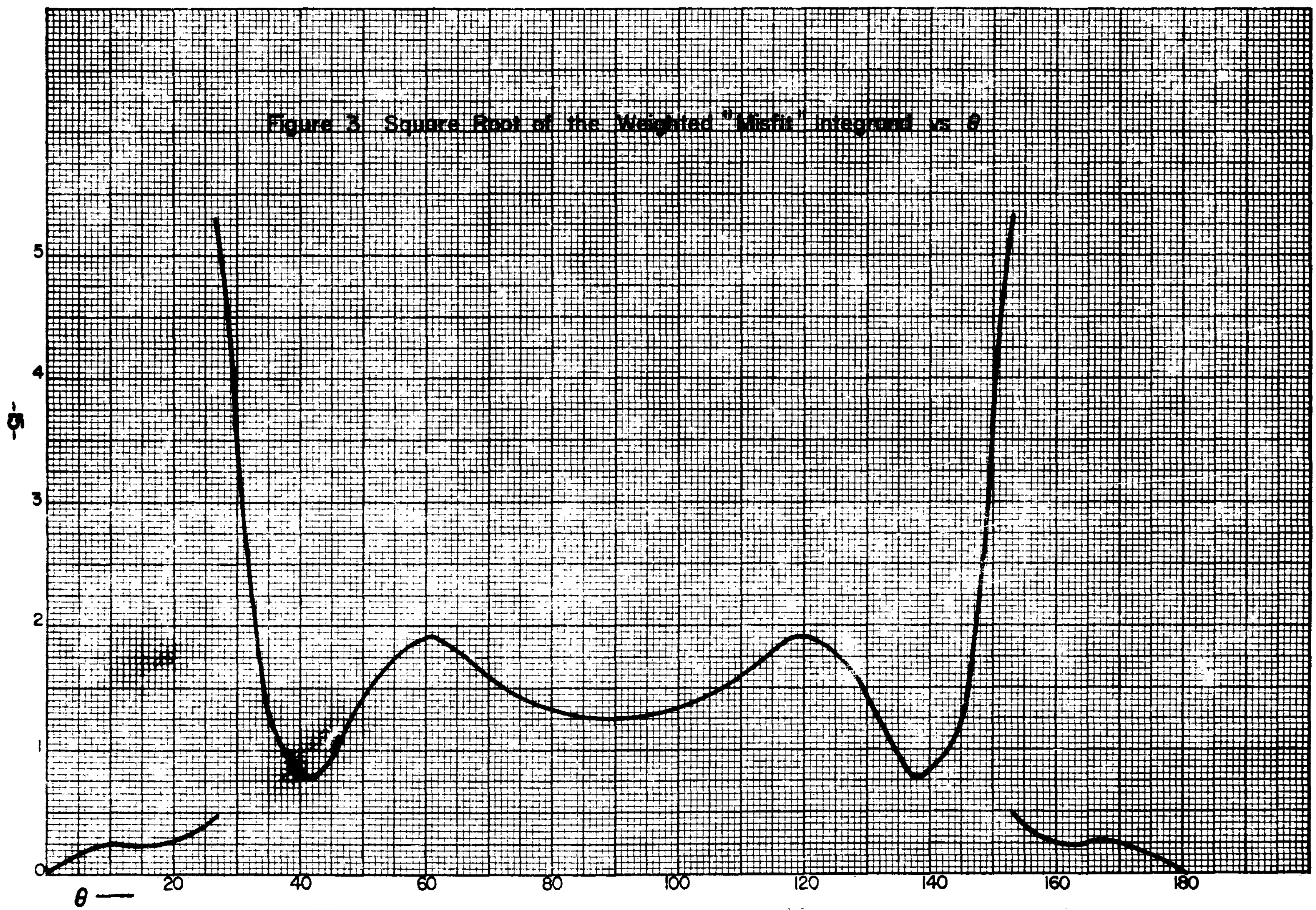

Figure 3. Square Root of the Weighted "Misfit" Integrand vs θ

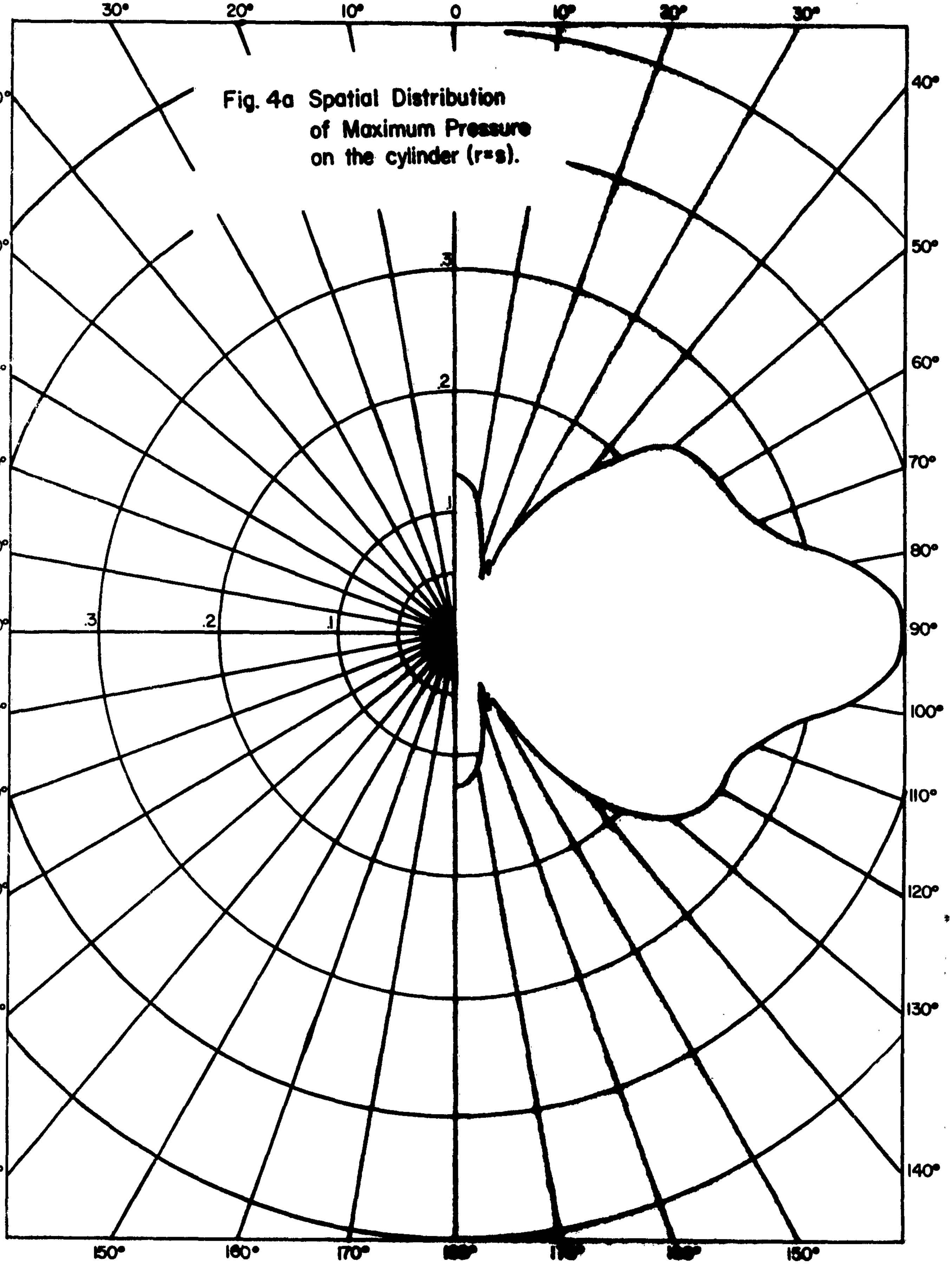
Fig. 4a Spatial Distribution
of Maximum Pressure
on the cylinder (r=s).
0
10°
20°
30°
40°
50°
60°
70°
80°
90°
100°
110°
120°
130°
140°
150°
160°
170°
180°
.1
.2
.3

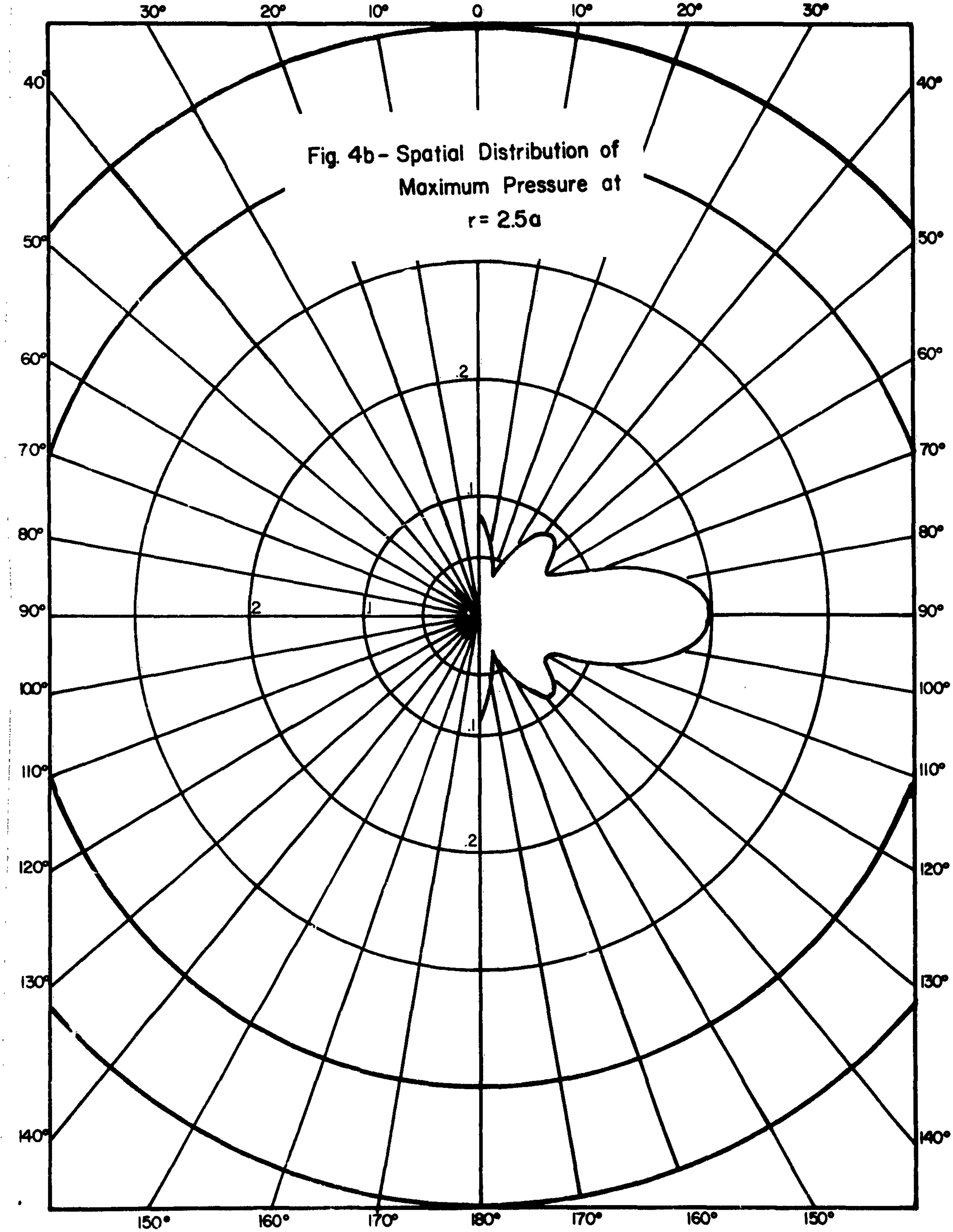

Fig. 4b - Spatial Distribution of Maximum Pressure at r = 2.5a

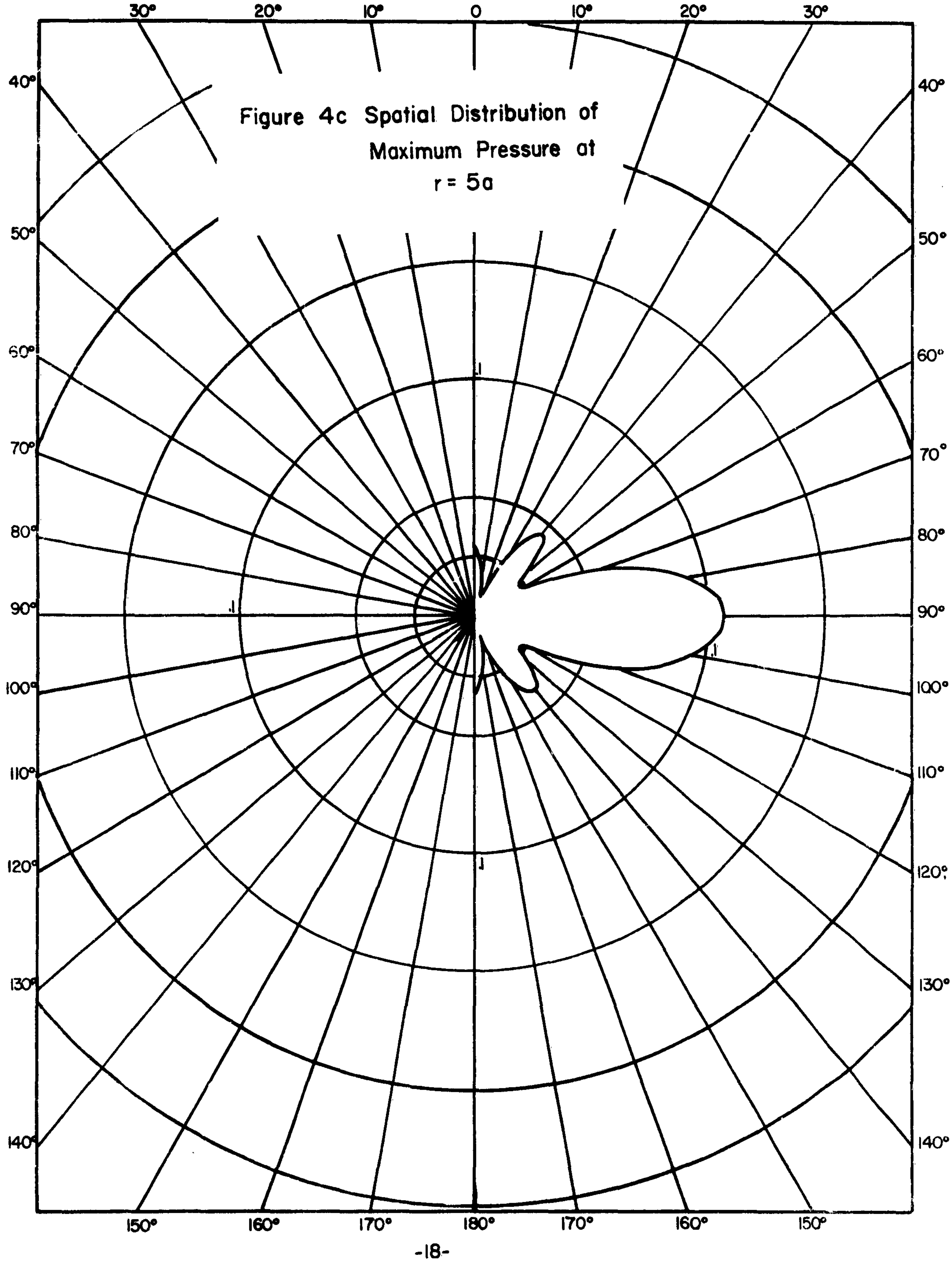

Figure 4c Spatial Distribution of Maximum Pressure at r = 5a

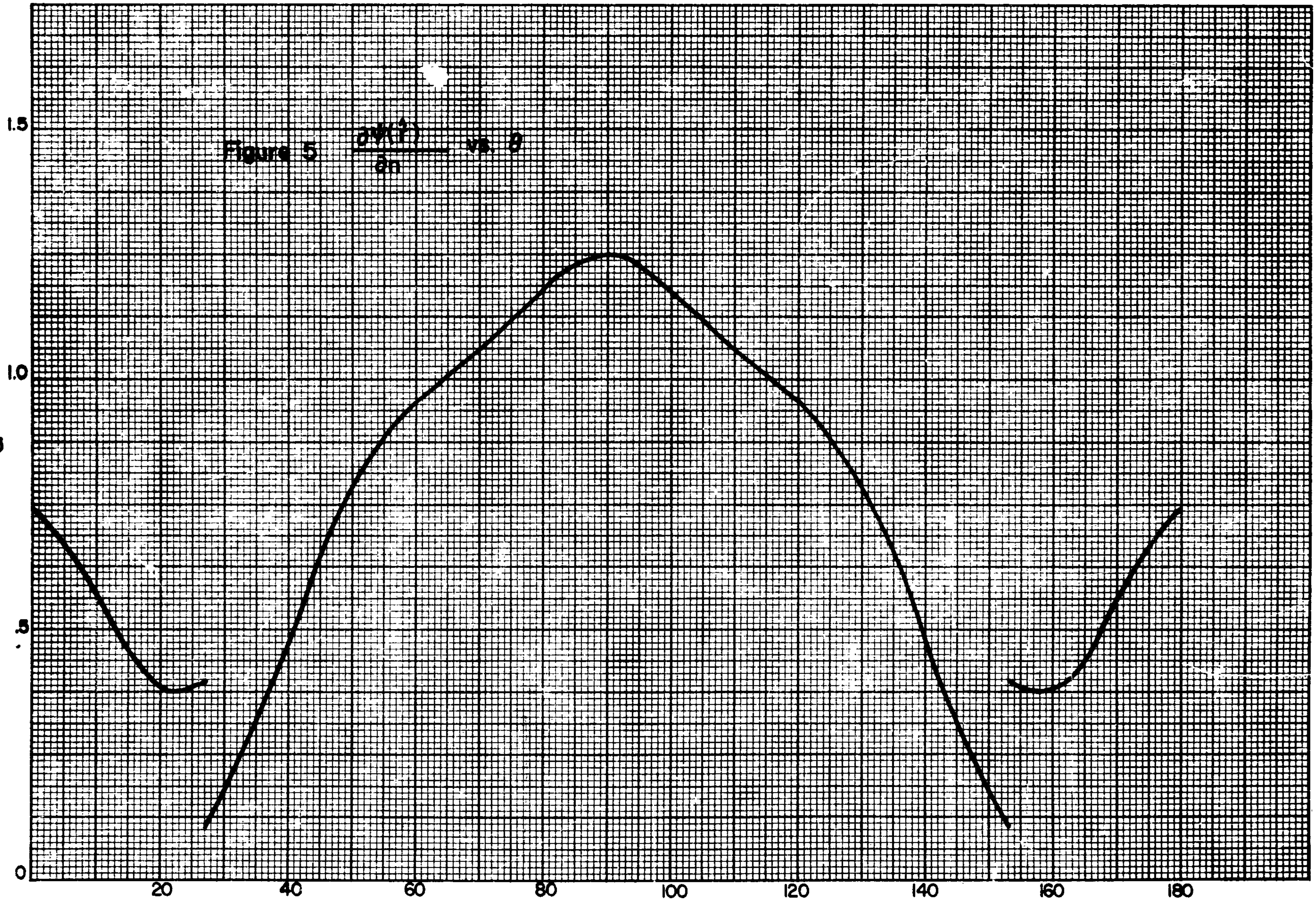

Figure 5 $\frac{\partial \psi(\hat{r})}{\partial n}$ vs. θ

"spike" follows not only from the crudity of the approximation but also, and more fundamentally, from the fact, which is emphasized in Figure 3, that the selection of the coefficients a_n was based not on minimizing the unweighted "misfit" with the attendant risk of having positive and negative "misfit" cancellation, but rather was based on minimizing the weighted squared misfit in analogy with the method by which orthogonal function expansions are matched to a given function[11].

<u>Remarks</u> - Because of the extensive numerical analysis required in carrying out the calculation outlined in the preceding section and because a primary desideratum of the calculation was its completion in a "finite" time, a less than ideal number of terms was employed in the series expansion. If the "rule of thumb" that the minimum highest order Hankel function in the series expansion should be $\sim 2ka - 3ka$ is applied to this specific problem, then $N = 10 - 15$ implies, at least, a 6 term expansion. Such an effort is close to, if not past, the economic break-even point for employment of an electronic data processing system <u>for this specific cylinder problem alone</u>. If, in addition, it is also recognized that a trivial change in the parameters a, b and ka requires a total recalculation, the employment of a high speed digital computer becomes mandatory.

By employing an electronic data processor it becomes feasible not only to perform lengthier calculations but also, because of this capability, it becomes feasible to postpone to a later stage of the calculation an undesirable feature which is imbedded in the structure of the current method. This limitation, which follows directly from the expansion of (18a) in terms of the non-orthogonal functions of (18b), leads to values for the coefficients a_n which are dependent on the number of terms employed in the series expansion. (This means, simply, that had a 4 term series expansion been selected for the numerical calculation of the previous section, say, the new values of a_1, a_2 and a_4 would differ, perhaps radically, from those in Table II calculated

---

[11] Although it is difficult, if not impossible to prove, it seems reasonable to expect that the expansion proposed in (22a) converges in the mean to H_2 except for possible spikes (analogous to the Gibbs phenomena) at the regional interfaces, as $N \to \infty$.

on the basis of a 3 term expansion.) This term dependence can be partially offset by means of the Gram-Schmidt Orthonormalization Process[12] which requires the use of a digital computer for its effective execution in this context.

This orthonormalization process and the resultant strengthening of the finite cylinder calculation is outlined as follows:

a) From the relations for the $f_n(\theta)$ of (18b) and (19) and the relation for s^2 of (15) construct the functions

(33) $$\phi_n(\theta) = f_n(\theta)/s^2 \quad .$$

b) From these non orthogonal functions $\phi_n(\theta)$ construct the orthonormal system $\eta_n(\theta)$ for the finite cylinder (relative to the weight function $W(\theta)$) by means of the prescription

(34a) $$\eta_0(\theta) = \phi_0(\theta)/\|\phi_0(\theta)\|$$

where $\|\phi_0(\theta)\|$ indicates the weighted norm of $\phi_0(\theta)$ and is defined by

(34b) $$\| \phi_0(\theta) \| = \left\{ \int_0^{\pi} \phi_0^*(\theta)\, \phi_0(\theta)\, W(\theta)\, d\theta \right\}^{1/2}$$

and

(35a) $$\eta_1(\theta) = \xi_1(\theta) / \|\xi_1(\theta)\|$$

in which

(35b) $$\xi_1(\theta) = \phi_1(\theta) - (\phi_1(\theta), \eta_0(\theta))\, \eta_0(\theta)$$

(12) cf. Lindsay, R.B. and Margenau, H., Foundations of Physics, John Wiley and Sons, Inc., 1936. pp.424-426.

where the inner product $(\phi_i(\theta), \eta_j(\theta))$ is defined by

(35c) $$(\phi_i(\theta), \eta_j(\theta)) = \int_0^{\pi} \phi_i^*(\theta)\eta_j(\theta)W(\theta)\,d\theta$$

and

(36a) $$\eta_2(\theta) = \xi_2(\theta)/\|\xi_2(\theta)\|$$

in which

(36b) $$\xi_2(\theta) = \phi_2(\theta) - (\phi_2(\theta), \eta_0(\theta))\eta_0(\theta) - (\phi_2(\theta), \eta_1(\theta))\eta_1(\theta)$$

and so forth until the required number of $\eta_n(\theta)$ have been calculated.

c) Replace the series expansion for $G(\theta)$ in (22) by

(37) $$G(\theta) \equiv \tilde{G}(\theta) = \sum_{n=0}^{N} b_n \eta_n(\theta)$$

where the $\eta_n(\theta)$ is the orthonormal set constructed by means of the Gram-Schmidt Process outlined in (34a), (35a) and (36).

d) Repeat the approximation analysis by minimizing the "misfit" integral

(38) $$E = \int_0^{\pi} [N(\theta) - \tilde{G}(\theta)]^2 W(\theta)\,d\theta$$

and noting that

(39) $$\int_0^{\pi} \eta_i^*(\theta)\eta_j(\theta) W(\theta)\,d\theta = \delta_{ij}$$

which is the orthonormalization condition guaranteed by the Gram-Schmidt Process; then

(40) $$b_n(\theta) = \int_0^{\pi} H_2 \eta_n^*(\theta) W(\theta)\,d\theta$$

which is term independent.

e) From (34a), (35b), (36b) and similarly formed relations for higher n, it is seen that the η's can be written as linear combinations of the ϕ's in the form

(41a) $$\eta_i(\theta) = \sum_{j=0}^{i} A_{ij}(\theta)\,\phi_j(\theta)$$

(where it should be noted that $A_{ij}(\theta)$ is a lower triangular matrix with $A_{ii} = 1/\|\xi_i\|$); hence, it follows from this and from (22a) and (37) that

(41b) $$\sum_{i=0}^{N} b_i\,\eta_i(\theta) = \sum_{i=0}^{N} b_i \sum_{j=0}^{i} A_{ij}(\theta)\phi_j(\theta) = \sum_{j=0}^{N} a_j\,\phi_j(\theta)$$

or, identifying appropriate terms

(42) $$a_j = \sum_{i=0}^{N} b_i\,A_{ij}$$

which is the required result for the a_j.

f) Consequently, the term dependence of the a_j's is introduced in such a way that a minimal amount of recalculation of previously determined a_j's is needed upon introducing an increased N, say $\underline{N}$, since adding $b_{N+1} A_{N+1,j} + \cdots + b_{\underline{N}} A_{\underline{N},j}$ to the a_j calculated for N terms satisfies the requirements of (42).

Arbitrary Finite Bodies of Revolution

This method of determining the velocity potential for the sound field associated with a finite cylinder is readily extended to arbitrary finite bodies of revolution. This is accomplished, simply, by determining the number of distinct regions and the extent of each in the polar angle θ for the cross sectional boundary of the body, introducing this number of H-functions such that each regional H-function is one within its region and zero otherwise, using these regional H-functions to construct the polar equation for the boundary and, finally, re-doing the analysis of this report by applying appropriate boundary conditions and introducing different weight functions (other than a uniform, areal weighting) when such changes are required by the needs of a specific problem.

NOTE ADDED IN PROOF: In the course of final editing, an error was unearthed in the numerical evaluation of the derivative of certain Legendre Polynomials. A cursory calculation indicates that the effect of this numerical error should change the numerical values cited for the a_n in Table II only moderately, thus preserving the form of the results exhibited in Figures 3, 4, and 5.

PARKE MATHEMATICAL LABORATORIES, INCORPORATED
BEDFORD ROAD • CARLISLE, MASSACHUSETTS

Distribution List

Organization	No. of Copies
Director Woods Hole Oceanographic Institute Woods Hole, Massachusetts	1
Director Acoustics Research Laboratory Harvard University Cambridge, Massachusetts	2
Director Acoustics Research Laboratory Massachusetts Institute of Technology Cambridge, Massachusetts	2
Director Marine Physical Laboratory Scripps Institute of Oceanography La Jolla, California	2
Inspector of Materials Applied Physics Laboratory University of Washington Seattle, Washington	1
Defense Research Laboratory University of Texas Austin 12, Texas	1
Hudson Laboratories Columbia University Dobbs Ferry, New York	1
Central Radio Propagation Laboratory National Bureau of Standards Washington, D. C.	1
Hans Jaffe, Director of Electronic Research Clevite Research Center 540 E. 105th Street Cleveland 8, Ohio	1

Distribution List Cont.

Organization	No. of Copies
Arch C. Scurlock, Research Director Atlantic Research Corporation Shirley Highway at Edsall Road Alexandria, Virginia	1
Director of Research Bell Telephone Laboratories Murray Hill, New Jersey	1
A. Finkelstein, Director of Research Stromberg Carlson Division General Dynamics Corporation Rochester, New York	1
Bendix Corporation Bendix - Pacific Division 11600 Sherman Way North Hollywood, California	1
H. B. Shaper, Director of Engineering Dyna - Empire, Inc. Dyna Laboratories 1075 Stewart Avenue Garden City, New York	1
C. Loda, Director of Research Edo Corporation 13-10 111th Street College Point, New York	1
John B. Russell, Manager Electronics Laboratory H. M. E. Dept. General Electric Company Syracuse, New York	1
Richard Mandelkorn, Vice-Pres. General Instrument Corporation Harris Transducer Division Main Street Woodbury, Connecticut	1
Frank Massa, Research Director Massa Division Cohn Electronics, Inc. 13 Fottler Road Hingham, Massachusetts	1

Distribution List Cont.

Organization	No. of Copies
Library Raytheon Company Willow Street Waltham 54, Massachusetts	1
Library Raytheon Company Wayland, Massachusetts	1
Library Raytheon Company Submarine Signal Division Portsmouth, Rhode Island	1
R. E. Grimm, Director of Engineering Vitro Corporation of America Nems - Clarke Company 919 Jesup - Blair Drive Silver Spring, Maryland	1
C. H. Lanphier, Director of Engineering Sangamo Electric Company 11th Street and Converse Avenue Springfield, Illinois	1
Mr. Samuel Hanish Naval Research Laboratory Washington 25, D. C.	1
Mr. Joshua Greenspon J. G. Engineering Research Associates Baltimore, Maryland	1
Mr. Ernst Prasse General Dynamics/Electronics 100 Carlson Road Rochester 3, New York	1
Mr. Satio Okada Stromberg Carlson Company 1400 Goodman Street Rochester 9, New York	1
Mr. Claude Horton Department of Physics University of Texas Austin 12, Texas	1

Distribution List Cont.

Organization	No. of Copies
Technical Director Contract N140-(70024)72788B U. S. Navy Underwater Sound Laboratory Fort Trumbull, New London, Connecticut Attn: Mr. Charles Sherman	3
U. S. Navy Purchasing Office 3rd Avenue and 29th Street Brooklyn 32, New York Attn: Mr. George F. Pucci	1
Chief of Naval Research Code 411 Department of the Navy Washington 25, D. C.	2
Chief of Naval Operations (OP-07T) Department of the Navy Washington 25, D. C.	2
Office of Technical Services Department of Commerce Washington, D. C.	1
Chief, Bureau of Ships Code 315 Department of the Navy Washington 25, D. C.	1
Chief, Bureau of Ships Code 320 Department of the Navy Washington 25, D. C.	1
Chief, Bureau of Ships Code 333 Department of the Navy Washington 25, D. C.	1
Chief, Bureau of Ships Code 335 Department of the Navy Washington 25, D. C.	3

Distribution List Cont.

Organization	No. of Copies
Chief, Bureau of Ships Code 688 Department of the Navy Washington 25, D. C.	1
Chief, Bureau of Ships Code 689A Department of the Navy Washington 25, D. C.	1
Chief, Bureau of Ships Code 689B Department of the Navy Washington 25, D. C.	1
Chief, Bureau of Ships Code 689C Department of the Navy Washington 25, D. C.	1
Chief, Bureau of Ships Code 689D Department of the Navy Washington 25, D. C.	1
Chief, Bureau of Ships Code 689E Department of the Navy Washington 25, D. C.	1
Commanding Officer U. S. Naval Ordinance Station Newport, Rhode Island	1
Officer in Charge Supreme Allied Commander Atlantic A.S.W. Research Center U. S. Naval Base Norfolk 11, Virginia	1
Commanding Officer and Director David Taylor Model Basin Washington 7, D. C.	2

Distribution List Cont.

Organization	No. of Copies
Commanding Officer and Director U. S. Naval Electronics Laboratory San Diego 52, California	2
Commanding Officer U. S. Navy Mine Defense Laboratory Panama City, Florida	1
Commanding Officer Air Force Cambridge Research Laboratory Air Research and Development Command Laurence G. Hanscom Field Bedford, Massachusetts	1
Commander U. S. Naval Air Development Center Johnsville, Pennsylvania	1
Commander U. S. Naval Ordinance Laboratory White Oak, Silver Spring Maryland	1
Commander Code 753 U. S. Naval Ordinance Test Station Inyoken, China Lake California	2
Commander Code 508 U. S. Naval Ordinance Test Station Inyoken, China Lake California	2
Commander U. S. Naval Ordinance Test Station Annex 3202 East Foothill Boulevard Pasadena 8, California	1
Director Naval Research Laboratory Washington 25, D. C.	2

Distribution List Cont.

Organization	No. of Copies
Director Ordinance Research Laboratory Pennsylvania State University University Park, Pennsylvania	2
Director U. S. Navy Underwater Sound Reference Laboratory Orlando, Florida	2
Commanding Officer and Director U. S. Naval Training Devise Center Port Washington Long Island, New York	1
Superintendant U. S. Navy Post Graduate School Monterey, California	1
Committee on Undersea Warfare National Research Council 2101 Constitution Avenue Washington, D. C.	1
ASTIA (TIPAA) Document Service Center Arlington Hall Station Arlington 12, Virginia	10
British Joint Services Mission Bureau of Ships Code 335 Department of the Navy Washington 25, D. C.	1
Canadian Joint Staff Bureau of Ships Code 335 Department of the Navy Washington 25, D. C.	1